

RESEARCH ARTICLE

View Article Online

View Journal | View Issue



Cite this: *Inorg. Chem. Front.*, 2021, **8**, 934

A hydrolytically stable Ce(IV) complex of glutarimide-dioxime†

Qiaomu Yang,^a Yusen Qiao,^a Alex McSkimming,^{‡a} Liane M. Moreau,^{§b} Thibault Cheisson,^a Corwin H. Booth,^b Ekaterina Lapsheva,^a Patrick J. Carroll^a and Eric J. Schelter^{a*}

The coordination chemistry of glutarimide-dioxime (H_3A) has been studied related to applications in uranyl sequestration from seawater and for the stabilization of early transition metals in high oxidation states. We report here that the H_2A^- anion is also suitable for stabilizing Ce(IV) and acts as a tridentate ligand to form the $[Ce(H_2A)_3]^+$ cation. The metal complexes $[Ce(H_2A)_3]Cl$ and $[Ce(H_2A)_3][BPh_4]$ have been obtained by oxidation of Ce(III) in the presence of H_3A under aerobic conditions. UV-Vis spectroscopy and DFT calculations were performed to characterize the electronic structure and ligand-to-metal charge transfer (LMCT) bands of $[Ce^{IV}(H_2A)_3]^+$. X-ray absorption spectroscopy (XAS) was also performed to verify the Ce(IV) oxidation state. Absent a clear electrochemical signal for cerium reduction in $[Ce(H_2A)_3]Cl$ or $[Ce(H_2A)_3][BPh_4]$ under a range of conditions, DFT calculations predicted a Ce(III/IV) redox couple of -1.22 V vs. Fc/Fc^+ . These results further expand the coordination chemistry of glutarimide-dioxime to tetravalent cerium.

Received 11th August 2020,
Accepted 4th December 2020

DOI: 10.1039/d0qi00969e

rs.c.li/frontiers-inorganic

Introduction

Among the lanthanides, the element cerium (Ce) can exhibit the unusual characteristic of a relatively accessible +4 oxidation state.^{1,2} To stabilize this high oxidation state, it is necessary to employ an electron-donating ligand that is resistant towards oxidation.^{3–8} There are a variety of reported Ce(IV) complexes stabilized by different ligand frameworks, such as $[NEt_4][CeCl_6]$, $[Ce(acac)_4]$, $[CeX(TrINOx)]$ ($TrINO_x^{3-} = [(2-^tBuNO)C_6H_4CH_2)_3N]^{3-}$; $X = F, Cl, Br$), $[Ce(pyNO)_4]$ ($pyNO = 2-(^tBuNO)pyridine$), and others.^{9–13} Glutarimide-dioxime (H_3A , $C_5H_9N_3O_2$), a compound reported to be useful for sequestering uranium from seawater, is considered here for stabilization of the cerium(IV) cation.

H_3A was originally known to extract uranyl ($U^{VI}O_2^{2+}$) as $[UO_2(HA)]$ and $[UO_2(H_2A)(HA)]^-$ from seawater, while compet-

ing with other uranyl species, such as $[UO_2(CO_3)_2]^{2-}$ and $[UO_2(CO_3)_3]^{4-}$.^{14–18} H_3A was then developed to readily chelate simple metal ions, such as $Ca(II)$,¹⁹ $Mg(II)$,¹⁹ $Cu(II)$,²⁰ $Pb(II)$,²⁰ $Ni(II)$,²⁰ $Mn(II)$,²¹ $Fe(III)$,²⁰ $Eu(III)$,²² $Nd(III)$,²² and metals of high oxidation states, such as $Th(IV)$,²³ $Np(IV)$,²³ $Pu(IV)$,²⁴ $Np(V)$,²⁵ and $V(V)$.^{26–28} We reasoned it would similarly stabilize the Ce(IV) cation as in the high oxidation state metal complexes cases (Scheme 1).

Complexation of glutarimide-dioxime (H_3A) with tetravalent cerium is of potential interest from applied and fundamental chemistry perspectives. A tetravalent cerium cation is expected to have a higher binding affinity with H_3A than trivalent lanthanides, which could facilitate lanthanide separations. From a fundamental standpoint, obtaining structural data, UV-Vis spectroscopic, and X-ray absorption spectra of a $Ln^{IV}-H_3A$ complex would allow the better understanding of the valency and ligand-to-metal charge transfer (LMCT) bands for Ln^{IV} complexes, and would provide an opportunity for comparison with the previously reported $An^{IV}-H_3A$ complex ($An = Th, Np, Pu$).^{23,24}

Results and discussion

Synthesis of $[Ce(H_2A)_3]Cl$ and $[Ce(H_2A)_3][BPh_4]$

Adding an aqueous solution of $Ce^{III}Cl_3$ to a prepared aqueous solution of 3 equiv. H_3A and 2 equiv. $NaOH$ in aerobic condition, resulted in an immediate colour change from colour-

^aP. Roy and Diana T. Vagelos Laboratories, Department of Chemistry, University of Pennsylvania, 231 South 34th Street, Philadelphia, Pennsylvania 19104, USA.

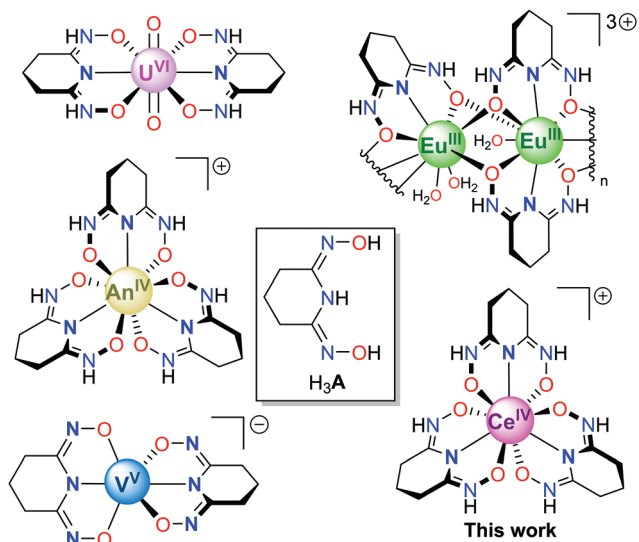
E-mail: schelter@sas.upenn.edu

^bChemical Sciences Division, Lawrence Berkeley National Laboratory, Berkeley, CA 94708, USA. E-mail: chbooth@lbl.gov

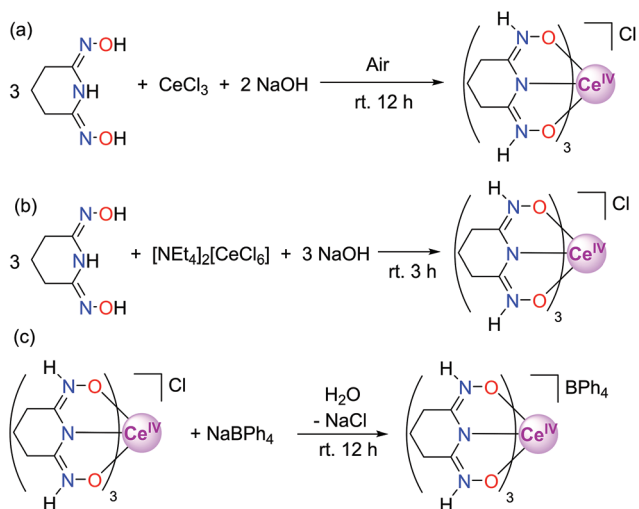
†Electronic supplementary information (ESI) available. CCDC 2015363 and 2015364. For ESI and crystallographic data in CIF or other electronic format see DOI: 10.1039/d0qi00969e

‡Current address: Department of Chemistry, Tulane University, New Orleans, LA 70118, USA. E-mail: ameskimming@tulane.edu

§Current address: Department of Chemistry, Washington State University, Pullman, WA 99164, USA. E-mail: liane.moreau@wsu.edu



Scheme 1 Glutarimide-dioxime (H_3A) and its complexes: $[\text{U}^{\text{VI}}\text{O}_2(\text{H}_2\text{A})_2]$, $[\text{Eu}^{\text{III}}(\text{H}_2\text{A})_3(\text{H}_2\text{O})_3(\text{ClO}_4)_3]$, $[\text{An}^{\text{IV}}(\text{H}_2\text{A})_3]$ ($\text{An} = \text{Th}, \text{Np}, \text{Pu}$), $[\text{V}^{\text{V}}\text{A}_2]^-$, and $[\text{Ce}^{\text{IV}}(\text{H}_2\text{A})_3]^+$ (this work).



Scheme 2 (a), (b) Synthesis of $[\text{Ce}^{\text{IV}}(\text{H}_2\text{A})_3] \text{Cl}$. (c) Synthesis of $[\text{Ce}(\text{H}_2\text{A})_3] [\text{BPh}_4]$.

less to first maroon and then purple (Scheme 2a). Oxidation of $\text{Ce}(\text{III})$ to $\text{Ce}(\text{IV})$ was strongly indicated by the presence of a characteristic LMCT band at 505 nm (Fig. S9†).¹⁰ Using $(\text{NEt}_4)_2[\text{CeCl}_6]$ as a $\text{Ce}(\text{IV})$ starting material with H_3A and NaOH in the proper stoichiometry, an identical purple solution was obtained and verified by ^1H NMR spectroscopy (Scheme 2b). ^1H NMR spectroscopy recorded on the purple solution in D_2O confirmed that the purple solution contained a new species, $[\text{Ce}(\text{H}_2\text{A})_3]\text{Cl}$.

The downfield chemical shift indicated a diamagnetic H_3A -based metal complex, consistent with previous reports (Fig. 1).²² Noting that the chemical shift of water is pH sensitive, we added trace acetone or Et_2O to the ^1H NMR sample to

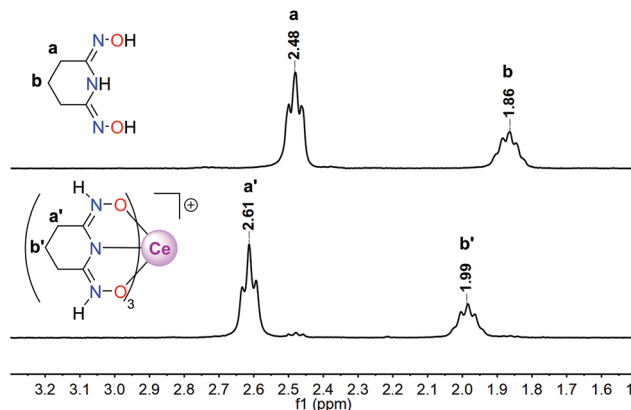


Fig. 1 ^1H NMR of H_3A and $[\text{Ce}(\text{H}_2\text{A})_3]^+$ in D_2O (300 MHz, room temperature). H_3A has shown the peaks at 2.48 and 1.86 ppm, while $[\text{Ce}(\text{H}_2\text{A})_3]^+$ has shown peak at 2.61 and 1.99 ppm.

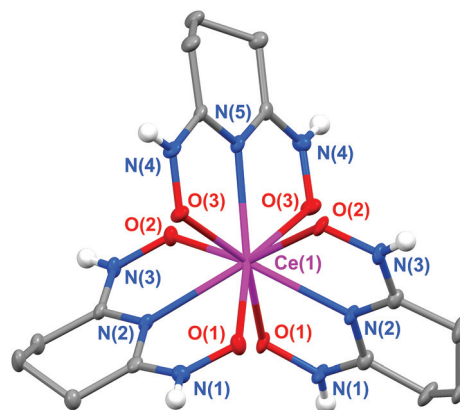


Fig. 2 Thermal ellipsoid plot of $[\text{Ce}(\text{H}_2\text{A})_3]\text{Cl}$ at 50% probability (Cl^- , aliphatic hydrogen atoms, and H_2O molecules are omitted for clarity).

act as an internal standard to obtain consistent results for H_3A and $[\text{Ce}(\text{H}_2\text{A})_3]^+$.

Purple needle-shaped crystals of $[\text{Ce}(\text{H}_2\text{A})_3]\text{Cl}$ were obtained by slow evaporation of an aqueous solution of the cerium(IV) complex (Fig. 2). The single crystal X-ray structure showed that $[\text{Ce}(\text{H}_2\text{A})_3]^+$ ions formed a 3-dimensional hydrogen bonding network with $=\text{N}(\text{O})\text{H}$ groups acting as proton donors and $\text{N}-\text{O}$ moieties functioning as proton acceptors, together with H_2O and Cl^- (see Fig. S2†).

Due to the low solubility of $[\text{Ce}(\text{H}_2\text{A})_3]\text{Cl}$ in organic solvents, a salt metathesis reaction was performed by adding an aqueous solution of NaBPh_4 to obtain a more organic soluble species (Scheme 2c). Chunks of purple crystals of $[\text{Ce}(\text{H}_2\text{A})_3][\text{BPh}_4]$ were obtained by recrystallization. The crystal structure of $[\text{Ce}(\text{H}_2\text{A})_3][\text{BPh}_4]$ showed that $[\text{Ce}(\text{H}_2\text{A})_3]^+$ ions formed a 2-dimensional hydrogen bonding network together with interstitial H_2O molecules. These 2-dimensional layers were separated by hydrophobic $[\text{BPh}_4]^-$ layers (see Fig. S4†).

Characterization and computational analysis

UV-visible absorption spectroscopy studies indicated that the purple colour of $[\text{Ce}(\text{H}_2\text{A})_3]\text{Cl}$ was due to a LMCT band at 505 nm (Fig. 3, a; $\epsilon = 2600 \text{ M}^{-1} \text{ cm}^{-1}$). Gaussian fits to the absorption band data yielded 3 bands at 228 nm, 284 nm and 487 nm (see Fig. S10†). The 228 nm band was assigned as a ligand-based transition considering the 228 nm absorption peak of the proligand.²⁹ The bands centred at 487 nm were assigned as LMCT bands, consistent with previous reports on other $\text{Ce}(\text{IV})$ systems.^{9,10}

To further understand the electronic transitions of the $[\text{Ce}(\text{H}_2\text{A})_3]^+$ cation, we have computed the electronic structure of $[\text{Ce}(\text{H}_2\text{A})_3]^+$ by density functional theory (DFT) and time-dependent density functional theory (TD-DFT) methods, based on the coordinates from the crystal structure. Similar calculations involving $\text{Ce}(\text{IV})$ or H_3A have been reported previously.^{16,21,28,30–32} The optimized structure exhibited good overall agreement with crystallographic data. The major differences involved the Ce–N bonds, exhibiting deviations up to 0.05 Å between the computational and experimental results. The highest occupied molecular orbital (HOMO) has a primarily ligand character (>98%) while the lowest unoccupied molecular orbitals (LUMO) has mostly Ce character (>97%), consistent with a highly ionic bonding interaction (Fig. 4).

TD-DFT calculations yielded vertical excitations within 3 major regions ~211, 261 and 510 nm. These corresponded to 3 transitions at 228 nm, 284 nm and 487 nm, obtained from a Gaussian fitting of the UV-visible spectrum (Fig. 3). As mentioned above, the first peak at 211 nm comprises transitions mostly from a C=N ($\pi \rightarrow \pi^*$) orbital, and transitions partially from a N–C–N π orbital to the Ce 4f orbitals. The second peak at 261 nm matches transitions from a C=N π orbital and a N–O π^* orbital to the C=N π^* orbital. The third transition at 510 nm denotes the transitions from a C=N π orbital and a N–O π^* orbital to the Ce 4f orbitals.

The third region of transitions was assigned between donors and acceptors: donors from HOMO–2 to HOMO of the ligand-based orbitals (>95%), and acceptors from LUMO to

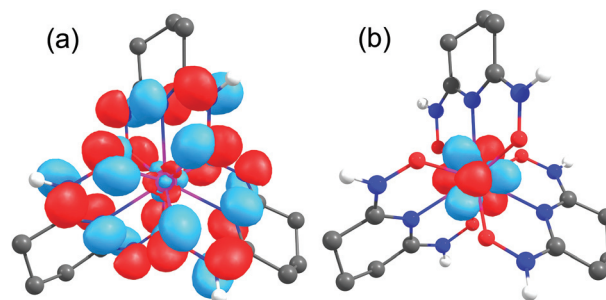


Fig. 4 (a) HOMO and (b) LUMO of $[\text{Ce}(\text{H}_2\text{A})_3]^+$ (protons attached to carbons are omitted for clarity).

LUMO+6 of the Ce 4f based orbitals (>92%) (see ESI Table S4†). Thus, the calculated transition at 510 nm can be assigned as a LMCT band.

Cerium(IV) compounds are known to exhibit valence instability and multiconfigurational ground state.³³ Thus, an X-ray absorption spectroscopic (XAS) experiment on the Ce L^{III} -absorption edge was performed to confirm the +4 oxidation state without valence instability and emphasize the ligand stabilizing ability. The spectrum showed 2 peaks indicative of the core hole excitation from a Ce(IV) ion of $2p_{3/2}4f^1\bar{\text{L}}5d^0$ and $2p_{3/2}4f^05d^0$ to the final states of $2p_{3/2}4f^1\bar{\text{L}}5d^1$ and $2p_{3/2}4f^05d^1$, where the bar indicates a hole (vacancy) and L indicates the ligand (Fig. 5). These data confirmed the expected +4 oxidation state of cerium within the complex. XANES fitting (see ESI†) revealed a fractional *f* occupancy (n_f) of 0.54(3), typical of formal Ce(IV) compounds.

To further evaluate the ligand stabilization of Ce(IV), we attempted to measure the redox potential of the Ce(III/IV) couple for the $[\text{Ce}(\text{H}_2\text{A})_3]^+$ cation. Solution cyclic voltammetry experiments were carried out for $[\text{Ce}(\text{H}_2\text{A})_3]\text{Cl}$ in H_2O using NaCl as supporting electrolyte and for $[\text{Ce}(\text{H}_2\text{A})_3][\text{BPh}_4]$ in $\text{CH}_3\text{CN}:\text{H}_2\text{O}$ (4:1 v/v) or propylene carbonate, both using $[\text{N}^n\text{Bu}_4]\text{PF}_6$ as supporting electrolyte. Notably, $[\text{Ce}(\text{H}_2\text{A})_3]\text{Cl}$ and $[\text{Ce}(\text{H}_2\text{A})_3][\text{BPh}_4]$ exhibited no obvious redox waves for Ce (III/IV) redox couple under these conditions. H_3A is known to lack electrochemical signals in its neutral state.²¹ The absence of a Ce(III/IV) redox wave in either case is somewhat unexpected, but self-consistent between the two different anions and sets

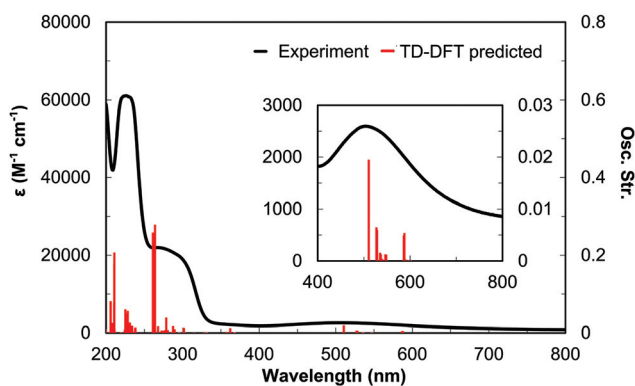


Fig. 3 UV-Vis spectrum and TD-DFT predicted oscillator strength of the $[\text{Ce}(\text{H}_2\text{A})_3]^+$ cation in H_2O . The inset showed the transition at 505 nm by zooming in, and all axes units were identical.

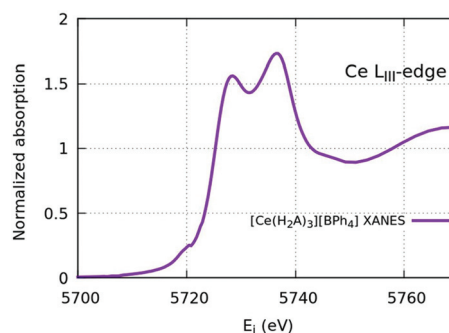


Fig. 5 X-ray absorption spectrum for $[\text{Ce}(\text{H}_2\text{A})_3][\text{BPh}_4]$.

of measurement conditions. The absence of Ce(III/IV) waves has been noted for other cerium complexes previously, including $\text{Ce}[\text{N}(\text{SiMe}_3)_2]_3$.³⁴ This phenomenon is tentatively attributed to slow kinetics of electron transfer from the sterically saturated Ce(III) complexes.^{34,35} Oxidation of Ce(III) complexes is typically accompanied by a reduction in cerium–ligand bonds of $\sim 0.1 \text{ \AA}$.³⁶ The slow electron transfer rate is thus attributed to a large inner sphere reorganization energy, as described by some of us previously.³⁵ Indeed, the only wave observed in the cyclic voltammetry experiments was an irreversible, BPh_4^- oxidation peak (see ESI†).

Although no wave corresponding to Ce(IV) reduction was detected in multiple trials in different solvents, DFT computation was used for a rough estimation of the cerium(III/IV) redox couple. This calculation method was used previously by us and shown to give good agreement with experimental values.^{30,31} Calculations for both $[\text{Ce}^{\text{IV}}(\text{H}_2\text{A})_3]^+$ and $[\text{Ce}^{\text{III}}(\text{H}_2\text{A})_3]$ were carried out using DCM as CPCM, B3LYP as the functional, ECP28MWB and 6-31G* as basis sets following previous reports.^{30,31} According to the total energy difference of $[\text{Ce}^{\text{IV}}(\text{H}_2\text{A})_3]^+$ and $[\text{Ce}^{\text{III}}(\text{H}_2\text{A})_3]$, the predicted redox potential was about -1.22 V vs. Fc/Fc^+ after calibration, which is relatively low compared with some cerium(IV) complexes, such as $[\text{N}^t\text{Bu}_4][\text{Ce}(\text{NO}_3)_6]$ (0.62 V), $\text{Ce}(\text{acac})_2$ (-0.38 V , $\text{acac} = \text{acetyl-acetate}$), $\text{Ce}(\text{OAr})_4$ (-0.50 V , $\text{OR} = 2,6\text{-diphenylphenol}$), $\text{Ce}(\text{OQ})_2$ (-0.61 V , $\text{OQ} = 8\text{-hydroxyquinolate}$) and $\text{Ce}(\text{OEP})_2$ (-1.06 V , $\text{OEP} = \text{octaethylporphyrin}$).^{30,31} This estimation indicates that H_2A^- is a good electron-donating ligand for stabilizing Ce(IV).

Attempts to obtain another redox isomer: $[\text{Ce}^{\text{III}}(\text{H}_2\text{A})_3]$, including mixing aqueous CeCl_3 , H_3A , and base under anaerobic condition, or reacting $\text{Ce}[\text{N}(\text{SiMe}_3)_2]_3$ with H_3A in organic solvents under an inert environment were attempted. While these reaction conditions have produced colorless or yellow solids respectively, as yet, no $[\text{Ce}^{\text{III}}(\text{H}_2\text{A})_3]$ complexes have been successfully isolated.

Experimental details

Materials and methods

1,6-Heptadiyne was purchased from Fisher Scientific. Deuterated water or acetonitrile were purchased from Cambridge Isotope Laboratories, Inc. CeCl_3 (>99.9% purity) was purchased from Strem. Glutarimide-dioxime (H_3A) was prepared and recrystallized using a known procedure.¹² Benchtop reactions were carried out under aerobic conditions. Reactions in anaerobic conditions were carried out using Schlenk techniques under N_2 atmosphere or in glovebox under N_2 atmosphere in attempts to prepare Ce(III) complexes.

Preparation of $[\text{Ce}(\text{H}_2\text{A})_3]\text{Cl}\cdot 3\text{H}_2\text{O}$

A H_2O (20 mL) solution of NaOH (27 mg, 0.67 mmol, 2 equiv.) was added into a H_2O (80 mL) solution of H_3A (143.2 mg, 1.00 mmol, 3 equiv.) in a round bottom flask with stirring. When all of the H_3A was dissolved, a 20 mL H_2O solution of

$\text{CeCl}_3\cdot 7\text{H}_2\text{O}$ (124.1 mg, 0.33 mmol, 1 equiv.) was added dropwise into the flask, and a purple solution appeared immediately. The reaction was allowed to react under aerobic conditions for 12 h. Anal. calcd for $\text{C}_{15}\text{H}_{24}\text{O}_6\text{N}_9\text{CeCl}$: C, 29.93; H, 4.02; N, 20.94. Found: C, 29.98; H, 4.10; N, 20.57. ^1H NMR (300 MHz, D_2O , room temperature) showed a yield of 81.3%, compared to $[\text{NMe}_4]\text{I}$ that was added as an internal standard. A solid yield was not obtained due to difficulties in crystallization, but the single crystals of X-ray quality were determined to be about 3% yield (6 mg) from slow evaporation of a saturated aqueous solution, with addition of several drops of saturated NaCl solution. ^1H NMR (300 MHz, D_2O , room temperature) δ : 1.98 (2H, $-\text{CH}_2-\text{CH}_2-\text{CH}_2-$), 2.61 (4H, $-\text{CH}_2-\text{CH}_2-\text{CH}_2-$). ^{13}C NMR (126 MHz, D_2O) δ : 17.45 ($-\text{CH}_2-\text{CH}_2-\text{CH}_2-$), 21.28 ($-\text{CH}_2-\text{CH}_2-\text{CH}_2-$), 157.81 ($-\text{C}=\text{N}=\text{OH}$). MS (ESI): $m/z = 423.1$ $[\text{Ce}(\text{H}_2\text{A})(\text{HA})]^+$, 143.1 $[\text{H}_4\text{A}]^+$.

Preparation of $[\text{Ce}(\text{H}_2\text{A})_3][\text{BPh}_4]$

An identical procedure was followed here for the preparation of $[\text{Ce}(\text{H}_2\text{A})_3]\text{Cl}\cdot 3\text{H}_2\text{O}$. After the H_2O solution of $[\text{Ce}(\text{H}_2\text{A})_3]\text{Cl}$ was prepared according to procedure above, a H_2O (20 mL) solution of NaBPh_4 (114.1 mg, 0.33 mmol, 1 equiv.) was added into the flask. Black solid precipitated out of solution immediately and was collected by filtration over a medium frit after reaction for 12 hours. The collected solid was redissolved in acetone: H_2O (2:1) mixture and then filtered through a medium frit. The filtrate was collected and evaporated to obtain X-ray quality crystals, yielding $[\text{Ce}(\text{H}_2\text{A})_3][\text{BPh}_4]\cdot 4\text{H}_2\text{O}$ in 53% yield for the whole reaction (180 mg). Anal. calcd for $\text{C}_{39}\text{H}_{52}\text{O}_{10}\text{N}_9\text{BCe}$: C, 48.91; H, 5.47; N, 13.16. Found: C, 48.89; H, 5.26; N, 12.80. Upon dissolution of $[\text{Ce}(\text{H}_2\text{A})_3][\text{BPh}_4]$ in $\text{CD}_3\text{CN}-\text{D}_2\text{O}$ (2:1) free proligand was always evident, indicating partial dissociation of H_2A^- from the complex (see ESI†). ^1H NMR (300 MHz, $\text{CD}_3\text{CN}:\text{D}_2\text{O} = 2:1$, room temperature) δ : 1.99 ($-\text{CH}_2-\text{CH}_2-\text{CH}_2-$); 2.49 ($-\text{CH}_2-\text{CH}_2-\text{CH}_2-$); 2.62 ($-\text{CH}_2-\text{CH}_2-\text{CH}_2-$); 6.93, 7.08, 7.35 (BPh_4^-). ^{13}C NMR (126 MHz, $\text{CD}_3\text{CN}:\text{D}_2\text{O} = 2:1$) δ : 18.64 ($-\text{CH}_2-\text{CH}_2-\text{CH}_2-$); 22.30 ($-\text{CH}_2-\text{CH}_2-\text{CH}_2-$); 158.21 ($-\text{C}=\text{N}=\text{OH}$); 122.85, 126.63, 126.65, 164.66 (BPh_4^-). MS (ESI): $m/z = 423.1$ $[\text{Ce}(\text{H}_2\text{A})(\text{HA})]^+$, 143.1 $[\text{H}_4\text{A}]^+$.

Characterization and computational analysis

^1H NMR spectra were obtained on a Bruker AM-500 or a Bruker UNI-300 Fourier transform NMR spectrometer at 500 or 300 MHz, respectively. $^{13}\text{C}\{^1\text{H}\}$ NMR spectra were recorded on a Bruker AM-500 Fourier transform NMR spectrometer at 126 MHz. Elemental analyses were obtained on a Costech ECS 4010 instrument at the Earth and Environmental Science department of the University of Pennsylvania. X-ray intensity data were collected on a Bruker APEXII CCD area detector or a Bruker APEXIII D8QUEST CMOS area detector, both employing graphite-monochromated $\text{MoK}\alpha$ radiation ($\lambda = 0.71073 \text{ \AA}$) at 100(1) K. UV-visible spectra were collected on a PerkinElmer 950 UV Vis/NIR spectrophotometer. Ce L_{III} -edge XANES data were collected at beamline 11-2 at the Stanford Synchrotron Radiation Lightsource. DFT and TD-DFT calculations were

carried out in Gaussian 09 Rev. A.02. In the DFT and TD-DFT calculation, we have employed cam-B3LYP-D3BJ as the functional in a H₂O CPCM as solvent continuum, ECP28MWB as an ECP for cerium and 6-311+G* as a general basis set. A second calculation employing B3LYP as the functional was also carried out for comparison and Ce(IV/III) redox couple prediction (see ESI†).

Conclusions

We have reported the cerium(IV) glutarimide dioxime complexes: [Ce(H₂A)₃]Cl and [Ce(H₂A)₃][BPh₄]. The compounds have been characterized by X-ray crystallography, NMR spectroscopy, UV-Vis spectroscopy and XANES. Solution electrochemical experiments did not reveal metal-based waves in either case. DFT calculations were used to assign the electronic structure and LMCT bands, and to estimate the Ce(IV) reduction potential -1.22 V *versus* Fc/Fc⁺. These studies expand the coordination chemistry of the glutarimide-dioxime compound amongst f-elements and cerium(IV) coordination chemistry to a new type of strongly-stabilized ligand environment.

Conflicts of interest

There are no conflicts to declare.

Acknowledgements

The authors gratefully acknowledge support from the University of Pennsylvania and the U.S. Department of Energy, Office of Science, Office of Basic Energy Sciences, Separation Science program under Award DE-SC0017259. Work at Lawrence Berkeley National Laboratory was supported by the Director, Office of Science, Office of Basic Energy Sciences, Division of Chemical Sciences, Geosciences, and Biosciences Heavy Element Chemistry Program of the U.S. Department of Energy (DOE) at LBNL under Contract No. DE-AC02-05CH11231. XANES measurements were performed at beamline 11-2 at the Stanford Synchrotron Radiation Lightsource, which is supported by the U.S. Department of Energy, Office of Science, Office of Basic Energy Sciences under contract no. DE-AC02-76SF00515. We also thank the U.S. Department of Energy, Office of Basic Energy Sciences under award DE-SC0020169 for partial support of E.L. This work used the Extreme Science and Engineering Discovery Environment (XSEDE), which is supported by NSF (ACI-1548562). We also thank Dr. Bren Cole for the beneficial discussion and editing of this manuscript.

Notes and references

- 1 P. F. Lang and B. C. J. Smith, Ionization energies of lanthanides, *Chem. Educ.*, 2010, **87**, 875–881.
- 2 L. J. Nugent, R. D. Baybarz, J. L. Burnett and J. L. Ryan, Electron-transfer and f → d absorption bands of some lanthanide and actinide complexes and the standard (III–IV) oxidation potentials for each member of the lanthanide and actinide series, *J. Inorg. Nucl. Chem.*, 1971, **33**, 2503–2530.
- 3 N. A. Piro, J. R. Robinson, P. J. Walsh and E. J. Schelter, The electrochemical behavior of cerium(III/IV) complexes: thermodynamics, kinetics and applications in synthesis, *Coord. Chem. Rev.*, 2014, **260**, 21–36.
- 4 N. T. Rice, I. A. Popov, D. R. Russo, T. P. Gomba, A. Ramanathan, J. Bacsá, E. R. Batista, P. Yang and H. S. La Pierre, Comparison of tetravalent cerium and terbium ions in a conserved, homoleptic imidophosphorane ligand field, *Chem. Sci.*, 2020, **11**, 6149–6159.
- 5 C. T. Palumbo, I. Zivkovic, R. Scopelliti and M. Mazzanti, Molecular complex of Tb in the +4 oxidation state, *J. Am. Chem. Soc.*, 2019, **141**, 9827–9831.
- 6 A. R. Willauer, C. T. Palumbo, R. Scopelliti, I. Zivkovic, I. Douair, L. Maron and M. Mazzanti, Stabilization of the oxidation state+ IV in siloxide-supported terbium compounds, *Angew. Chem., Int. Ed.*, 2020, **59**, 3549–3553.
- 7 A. R. Willauer, C. T. Palumbo, F. Fadaei-Tirani, I. Zivkovic, I. Douair, L. Maron and M. Mazzanti, Accessing the +IV oxidation state in molecular complexes of praseodymium, *J. Am. Chem. Soc.*, 2020, **142**, 5538–5542.
- 8 T. P. Gomba, A. Ramanathan, N. T. Rice and H. S. La Pierre, The chemical and physical properties of tetravalent lanthanides: Pr, Nd, Tb, and Dy, *Dalton Trans.*, 2020, **49**, 15945–15987.
- 9 H. L. Yin, Y. Jin, J. E. Hertzog, K. C. Mullane, P. J. Carroll, B. C. Manor, J. M. Anna and E. J. Schelter, The hexachloro-cerate(III) anion: a potent, benchtop stable, and readily available ultraviolet A photosensitizer for aryl chlorides, *J. Am. Chem. Soc.*, 2016, **138**(50), 16266–16273.
- 10 Y. Qiao and E. J. Schelter, Lanthanide photocatalysis, *Acc. Chem. Res.*, 2018, **51**, 2926–2936.
- 11 J. A. Bogart, C. A. Lippincott, P. J. Carroll, C. H. Booth and E. J. Schelter, Controlled redox chemistry at cerium within a tripodal nitroxide ligand framework, *Chem. – Eur. J.*, 2015, **21**, 17850–17859.
- 12 J. A. Bogart, A. J. Lewis, S. A. Medling, N. A. Piro, P. J. Carroll and E. J. Schelter, Homoleptic cerium(III) and cerium(IV) nitroxide complexes: significant stabilization of the 4+ oxidation state, *Inorg. Chem.*, 2013, **52**, 11600–11607.
- 13 N. T. Rice, J. Su, T. P. Gomba, D. R. Russo, J. Telser, L. Palatinus, J. Bacsá, P. Yang, E. R. Batista and H. S. La Pierre, Homoleptic imidophosphorane stabilization of tetravalent cerium, *Inorg. Chem.*, 2019, **58**, 5289–5304.
- 14 C. J. Leggett, F. Endrizzi and L. Rao, Scientific basis for efficient extraction of uranium from seawater, II: fundamental thermodynamic and structural studies, *Ind. Eng. Chem. Res.*, 2016, **55**, 4257–4263.
- 15 G. Tian, S. J. Teat, Z. Zhang and L. Rao, Sequestering uranium from seawater: binding strength and modes of

- uranyl complexes with glutarimidedioxime, *Dalton Trans.*, 2012, **41**, 11579–11586.
- 16 S. Chatterjee, V. S. Bryantsev, S. Brown, J. C. Johnson, C. D. Grant, R. T. Mayes, B. P. Hay, S. Dai and T. Saito, Synthesis of naphthalimidedioxime ligand-containing fibers for uranium adsorption from seawater, *Ind. Eng. Chem. Res.*, 2016, **55**, 4161–4169.
 - 17 X. Sun, G. Tian, C. Xu, L. Rao, S. Vukovic, S. O. Kang and B. P. Hay, Quantifying the binding strength of U(VI) with phthalimidedioxime in comparison with glutarimidedioxime, *Dalton Trans.*, 2014, **43**, 551–557.
 - 18 C. W. Abney, R. T. Mayes, T. Saito and S. Dai, Materials for the recovery of uranium from seawater, *Chem. Rev.*, 2017, **117**, 13935–14013.
 - 19 C. J. Leggett and L. Rao, Complexation of calcium and magnesium with glutarimidedioxime: implications for the extraction of uranium from seawater, *Polyhedron*, 2015, **95**, 54–59.
 - 20 X. Sun, C. Xu, G. Tian and L. Rao, Complexation of glutarimidedioxime with Fe(III), Cu(II), Pb(II), and Ni(II), the competing ions for the sequestration of U(VI) from seawater, *Dalton Trans.*, 2013, **42**, 14621–14627.
 - 21 X. Xie, Y. Tian, Z. Qin, Q. Yu, H. Wei, D. Wang, X. Li and X. Wang, Complexation of manganese with glutarimidedioxime: Implication for extraction uranium from seawater, *Sci. Rep.*, 2017, **7**, 43503.
 - 22 S. A. Ansari, Y. Yang, Z. Zhang, K. J. Gagnon, S. J. Teat, S. Luo and L. Rao, Complexation of lanthanides with glutaroimide-dioxime: binding strength and coordination modes, *Inorg. Chem.*, 2016, **55**, 1315–1323.
 - 23 Z. Zhang, B. F. Parker, T. D. Lohrey, S. J. Teat, J. Arnold and L. Rao, Complexation-assisted reduction: complexes of glutaroimide-dioxime with tetravalent actinides (Np(IV) and Th(IV)), *Dalton Trans.*, 2018, **47**, 8134–8141.
 - 24 L. Xian, G. Tian, C. M. Beavers, S. J. Teat and D. K. Shuh, Glutarimidedioxime: A complexing and reducing reagent for plutonium recovery from spent nuclear fuel reprocessing, *Angew. Chem., Int. Ed.*, 2016, **55**, 4671–4673.
 - 25 S. A. Ansari, A. Bhattacharyya, Z. Zhang and L. Rao, Complexation of neptunium(V) with glutaroimide dioxime: A study by absorption spectroscopy, microcalorimetry, and density functional theory calculations, *Inorg. Chem.*, 2015, **54**, 8693–8698.
 - 26 C. J. Leggett, B. F. Parker, S. J. Zhang, P. D. Dau, W. W. Lukens, S. M. Peterson, A. J. P. Cardenas, M. G. Warner, J. K. Gibson, J. Arnold and L. Rao, Structural and spectroscopic studies of a rare nonoxido V(V) complex crystallized from aqueous solution, *Chem. Sci.*, 2016, **7**, 2775–2786.
 - 27 A. S. Ivanov, C. J. Leggett, B. F. Parker, Z. Zhang, J. Arnold, S. Dai, C. W. Abney, V. S. Bryantsev and L. Rao, Origin of the unusually strong and selective binding of vanadium by polyamidoximes in seawater, *Nat. Commun.*, 2017, **8**, 1560.
 - 28 D. Sanna, V. Ugone, G. Sciortino, B. F. Parker, Z. Zhang, C. J. Leggett, J. Arnold, L. Rao and E. Garribba, VIVO and VIV species formed in aqueous solution by the tridentate glutaroimide-dioxime ligand – an instrumental and computational characterization, *Eur. J. Inorg. Chem.*, 2018, **17**, 1805–1816.
 - 29 J. A. Elvidge, R. P. Linstead and A. M. Salaman, Heterocyclic imines and amines. Part IX. Glutarimidine and the imidine from α -phenylglutaronitrile, *J. Chem. Soc.*, 1959, **37**, 208–215.
 - 30 J. R. Levin, W. L. Dorfner, A. X. Dai, P. J. Carroll and E. J. Schelter, Density functional theory as a predictive tool for cerium redox properties in nonaqueous solvents, *Inorg. Chem.*, 2016, **55**, 12651–12659.
 - 31 J. A. Bogart, A. J. Lewis, M. A. Boreen, H. B. Lee, S. A. Medling, P. J. Carroll, C. H. Booth and E. J. Schelter, A ligand field series for the 4f-Block from experimental and DFT computed Ce(IV/III) electrochemical potentials, *Inorg. Chem.*, 2015, **54**, 2830–2837.
 - 32 Y. Qiao, T. Cheisson, B. C. Manor, P. J. Carroll and E. J. Schelter, A strategy to improve the performance of cerium(III) photocatalysts, *Chem. Commun.*, 2019, **55**, 4067–4070.
 - 33 C. H. Booth, M. D. Walter, M. Daniel, W. W. Lukens and R. A. Andersen, Self-contained kondo effect in single molecules, *Phys. Rev. Lett.*, 2005, **95**, 267202.
 - 34 J. R. Robinson, P. J. Carroll, P. J. Walsh and E. J. Schelter, The impact of ligand reorganization on cerium(III) oxidation chemistry, *Angew. Chem., Int. Ed.*, 2012, **51**, 10159–10163.
 - 35 J. R. Robinson, Z. Gordon, C. H. Booth, P. J. Carroll, P. J. Walsh and E. J. Schelter, Tuning reactivity and electronic properties through ligand reorganization within a cerium heterobimetallic framework, *J. Am. Chem. Soc.*, 2013, **135**, 19016–19024.
 - 36 R. D. Shannon, Revised effective ionic radii and systematic studies of interatomic distances in halides and chalcogenides, *Acta Crystallogr.*, 1976, **A32**, 751–767.